

## 26.9 A 0.038mm<sup>2</sup> SAW-less Multiband Transceiver Using an N-Path SC Gain Loop

Gengzhen Qi<sup>1</sup>, Pui-In Mak<sup>1</sup>, Rui P. Martins<sup>1,2</sup>

<sup>1</sup>University of Macau, Macau, China,

<sup>2</sup>Instituto Superior Tecnico, Lisbon, Portugal

N-path filtering has been intensely rekindled as a replacement of costly SAW filters, making possible of multiband blocker-tolerant receivers (RXs) at small area and power, e.g., [1]. This paper proposes an *N-Path Switched-Capacitor (SC) Gain Loop* that is reconfigurable as an RF-tunable transmitter (TX) or RX with LO-defined center frequency. Comparatively, a SAW-less RX should be able to amplify a weak in-band (IB) signal in the presence of large out-of-band (OB) blockers, whereas a SAW-less TX should be able to deliver a large IB signal with low spectral leakage and OB noise. Such discrepancy inspires exploration of an *RX-TX-compatible N-path technique* to realize a multiband transceiver (TXR) with zero on-chip inductors and external matching components. Our TXR aims at the multiband LTE standard, and comparable performances are achieved at a die size 24x smaller than the recent art [2, 3].

The proposed *SC-Gain Loop* (Fig. 26.9.1a) is a negative-gain stage with an SC network as its feedback. Any signals, RF or BB, properly injected into the loop will undergo *gain*, *downmix* and *upmix*; all are primary functions of TX or RX. Thus, the SC-gain loop can operate as a basic TX by injecting the BB signal while extracting the RF signal (Fig. 26.9.1b), or a basic RX by injecting the RF signal while extracting the BB signal (Fig. 26.9.1c). This duality suggests the possibility of using the SC-gain loop as a reconfigurable TXR appropriate for LTE-TDD. Elegantly, the extra downmix path in the TX and upmix path in the RX allow the SC-gain loop to effectively combine with the *gain-boosted N-path technique* [4] to realize LO-defined high-Q bandpass (de)modulation, as described next.

To interface with the typical 4-phase BB signals (I/Q and differential) for quadrature modulation, a *4-path SC-gain loop* can become a practical TX (Fig. 26.9.2).  $V_{BB,TX1-4}$  are injected via passive-RC filters ( $R_{BT}$  and  $C_{BT}$ ) that also suppress the OB noise of the BB sources (e.g., DACs). As the N-path filter ( $C_F$  and  $SW_{L,R}$ ) is created around the gain stage ( $G_{m,RF}$ ), high-Q bandpass filtering is created at both  $V_{i,TX}$  and  $V_{o,TX}$  [4]. The loop gain offered by  $G_{m,RF}$  reduces the required size of  $C_F$  (8pF) thanks to the Miller multiplication effect, and decouples the size of  $SW_{L,R}$  to the OB rejection (i.e., smaller LO power).

Unlike the RX-only N-path solution in [1] that benefits from a large  $G_{m,RF}$  (200mS) to improve the NF and OB linearity, the concerns of spectral regrowth and EVM for our TX mode restrict the extent of  $G_{m,RF}$  (130mS). Also, in order to decouple the signal-handling ability of  $G_{m,RF}$  to the overall TX output power,  $V_{o,TX}$  is further amplified by a high-input-impedance PA driver (PAD) before driving the off-chip 50Ω load. The single-ended push-pull PAD is power efficient and offers a wide 1dB output bandwidth (~2.1GHz) adequate to cover >80% of the LTE bands from 0.7 to 2GHz. From noise simulations, the PAD contributes only 10% of the total OB noise (-157.7dBm/Hz) at 80MHz offset, which is indeed dominated by  $R_{BT}$  (24%),  $G_{m,RF}$  (20%) and  $SW_{L,R}$  + LO div-by-4 (20%). The rest comes from the 50Ω load and switches  $SW_{TX,RX}$  for TX-RX mode control.

When the extra downmix path in Fig. 26.9.2 is omitted, our closed-loop TX returns to an open-loop style similar to [5] that aims at low OB noise emission by direct quadrature-voltage modulation. The key difference here is that the gain created by  $G_{m,RF}$  is recycled to boost the Q of the bandpass responses at  $V_{i,TX}$  and  $V_{o,TX}$  as compared in Fig. 26.9.3a, rejecting the OB noise effectively.

The size of  $R_{BT}$  plays a key role in balancing the overall performance. As any resistors added to the N-path SC-gain loop can degrade the Q at  $V_{i,TX}$  and  $V_{o,TX}$ , a large  $R_{BT}$  benefits the OB rejection but at the expense of certain passband gain due to the finite input impedance at  $V_{i,TX}$  (Fig. 29.6.3b). In fact, as  $R_{BT}$  incurs noise as well, the rejection of OB noise will eventually saturate when enlarging only  $R_{BT}$  (Fig. 29.6.3c). For the spectrum purity,  $V_{o,TX}$  contains typical LO harmonic emission with  $HRR_3=9.5dB$  for  $N=4$ . Nevertheless, with the limited bandwidth of the PAD and output pad (bondwire), the  $HRR_3$  at the TX output  $V_{RF,TX}$  is improved (Fig. 29.6.3d), and goes up with frequency (e.g., 23dB at 2GHz). The  $HD_2$  at  $V_{RF,TX}$  is dominated by the single-ended PAD, and it is <-37dBc at a 0dBm output in simulations (Fig. 26.9.3d), by properly matching the PAD's push-pull transistors. Note that the commercial high-power LTE PA (e.g., [6]) is narrowband and will

suppress all OB harmonics from its TX. Thus, the final spectrum should still be dominated by the PA harmonic distortion [6].

The 4-path SC-gain loop can embody as a multiband RX for differential I/Q demodulation using no off-chip matching (Fig. 29.6.4). The source port is injected at  $V_{i,RX}$ , where a bandpass input impedance is created by frequency-translating the BB lowpass response (~10MHz, defined by  $R_{BR}C_{BR}$ ) to RF as bandpass, via the passive mixer  $SW_L$ . Note that  $SW_L$  +  $C_F$  already embed the downmix function saving one side of mixers [1]. Thanks to the loop gain created by  $G_{m,RF}$ , the BB circuitry sees a higher impedance back to the source port, allowing large  $R_{BR}$  (21kΩ) and small  $C_{BR}$  (1pF) to reduce the die area. Additionally, as  $R_F$  is no longer handicapped by the input-impedance matching, a large  $R_F$  (9.3kΩ) concurrently benefits the RF-to-BB gain, NF and OB rejection.

For the BB extraction, unlike [1] that uses resistors, here switches  $SW_0$  are employed (Fig. 29.6.4).  $SW_0$  and  $SW_L$  share the same set of 25%-duty-cycle LO, but are out-phased with each other. This undertaking obviates the BB noise from leaking directly to the source port, resulting in >1dB better simulated NF at 2GHz when comparing with [1].

The TXR fabricated in 65nm CMOS has a die area of 0.038mm<sup>2</sup> dominated by the capacitors (48pF) and PAD. The RF-input bandwidth is set at 10MHz to support the LTE10, and is adjustable via  $R_{BT}$  (Fig. 29.6.3b). Both  $G_{m,RF}$  and  $G_{m,BB}$  are inverter-based amplifiers to enhance the  $g_m$ /current efficiency. The LO generator is a div-by-4 measuring an average power efficiency of 6.6mW/GHz. At 2GHz, its simulated phase noise is -159.8dBc/Hz at 80MHz offset.

For the TX mode, the  $P_{out}$  shows -1dBm at 1.88GHz (Band2) after de-embedding the cable and PCB loss. The  $ACLR_1$  ( $ACLR_2$ ) is -40dBc (-51.9dBc) (Fig. 29.6.5a) and EVM is 2.0%. The output noise floor is -154.5dBc/Hz at 80MHz offset and  $CIM_3$  is -52dBc. The results are similar at 0.836GHz (Band5) and are summarized in Fig. 29.6.6. High-Q bandpass characteristics are consistently measured at different RF, by simply sweeping the LO frequency (Fig. 29.6.5b). The TX-mode consumes 31.3mW (Band5) to 38.4mW (Band2) (Fig. 29.6.5c).

For the RX mode, the  $S_{11}$  is <-12dB. The NF is 2.2dB at Band5, and up to 3.2dB at Band2 limited by the bondwire effects. Unlike [1] that targets a narrow RF BW (2.7MHz), here the RF BW is much wider (10MHz) and therefore the achieved OB- $P_{1dB}$  (-5dBm) and OB-IIP3 (+8dBm) are both competitive at 80MHz offset. The 0dBm-blocker NF is 16dB at 80MHz offset.

Benchmarking with the recent LTE TXs [2,3], our TRX in TX mode succeeds in creating multiband flexibility, while achieving a comparable TX efficiency at a much smaller die size. For our TRX in RX mode, similar NF and die size are achieved when comparing with [1], while this work operates at 1.25x higher RF and entails only a single supply (Fig. 29.6.7).

### Acknowledgements:

The authors thank Macao FDCT and UM-MYRG2015-00040-FST for financial support and Dr. Zhicheng Lin for discussion on the receiver mode.

### References:

- [1] Z. Lin, P.-I. Mak and R. P. Martins, "A 0.028mm<sup>2</sup> 11mW single-mixing blocker-tolerant receiver with double-RF N-path filtering,  $S_{11}$  centering, +13dBm OB-IIP3 and 1.5-to-2.9dB NF," *ISSCC Dig. Tech. Papers*, pp. 36-37, Feb. 2015.
- [2] Y.-H. Chen, N. Fong, B. Xu and C. Wang, "An LTE SAW-less Transmitter Using 33% Duty-Cycle LO Signals for Harmonic Suppression," *ISSCC Dig. Tech. Papers*, pp. 172-173, Feb. 2015.
- [3] N. Codega, P. Rossi, A. Pirola, A. Liscidini and R. Castello, "A current-mode, low out-of-band noise LTE transmitter with a class-A/B power mixer," *IEEE J. Solid-State Circuits*, vol. 49, pp. 1627-1638, July 2014.
- [4] Z. Lin, P.-I. Mak and R. P. Martins, "A 0.5V 1.15mW 0.2mm<sup>2</sup> sub-GHz ZigBee receiver supporting 433/860/915/960MHz ISM bands with zero external components," *ISSCC Dig. Tech. Papers*, pp. 164-165, Feb. 2014.
- [5] X. He and J. van Sinderen, "A 45nm low-power SAW-Less WCDMA transmit modulator using direct quadrature voltage modulation," *ISSCC Dig. Tech. Papers*, pp. 120-121, Feb. 2009.
- [6] Anadigics LTE Power Amplifier (AWT6652).

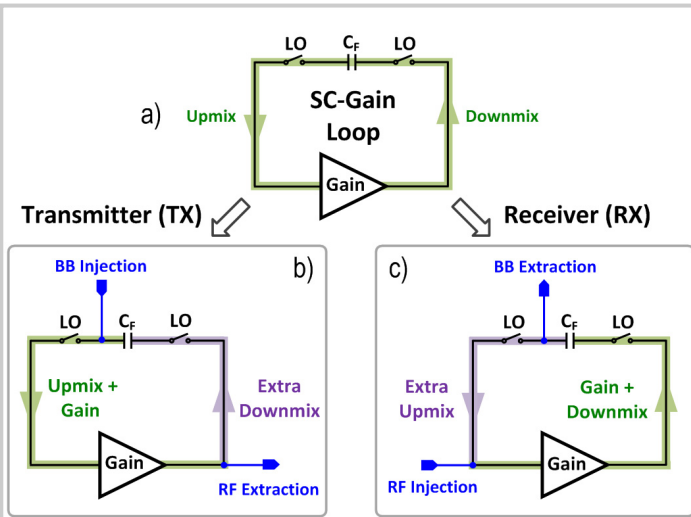


Figure 26.9.1: a) SC-Gain Loop. It can operate as b) TX under BB-injection RF-extraction, or c) RX under RF-injection BB-extraction.

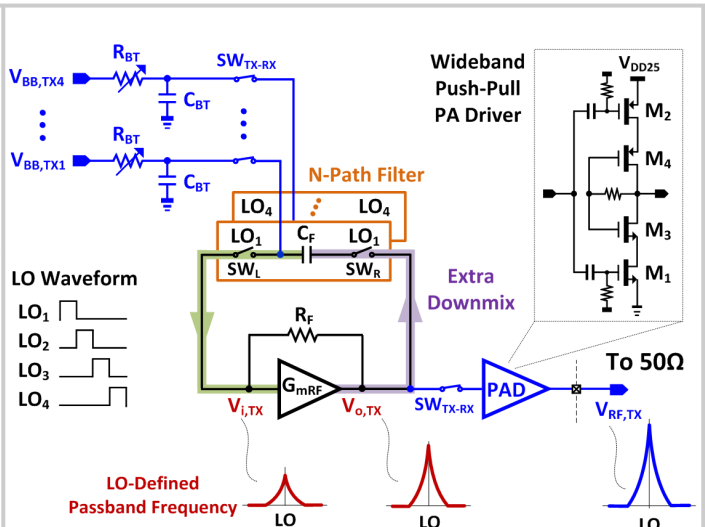


Figure 26.9.2: 4-Path SC-Gain Loop as a TX.

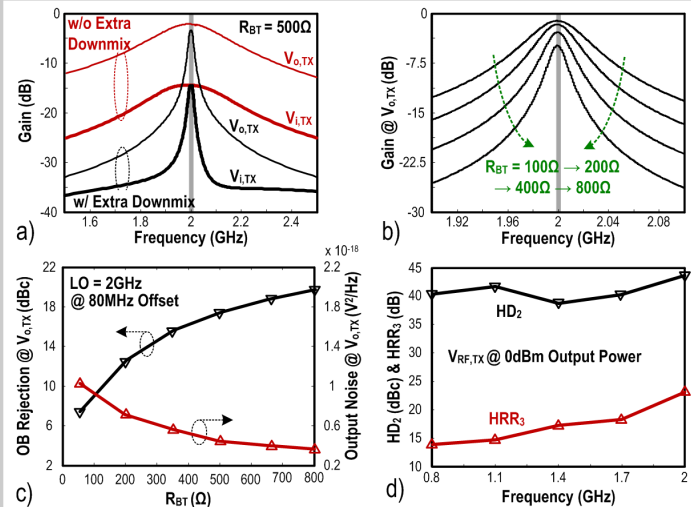


Figure 26.9.3: Simulated TX-mode performances at 2GHz: a)  $V_{i,TX}$  and  $V_{o,TX}$ ; b)-c)  $R_{BT}$  controls the RF BW, stopband rejection and output noise; d) OB harmonics of  $V_{RF,TX}$  at 0dBm output.

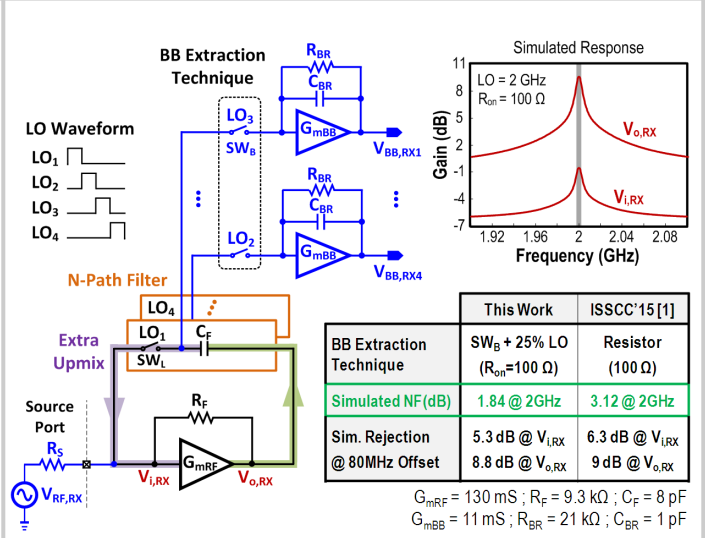


Figure 26.9.4: 4-path SC-Gain Loop as an RX.

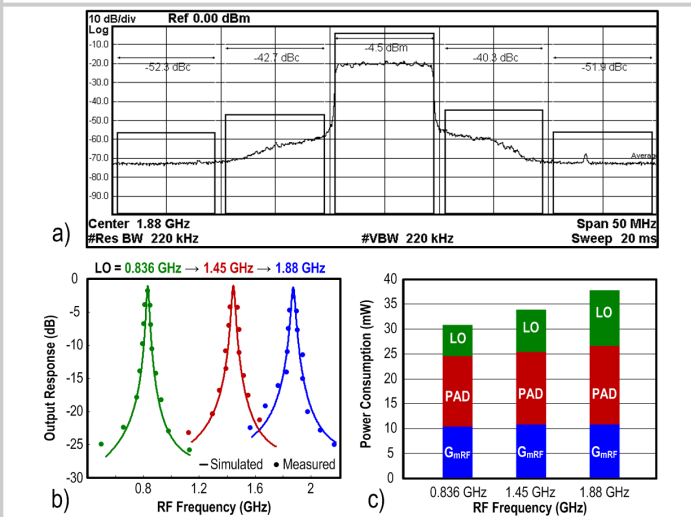


Figure 26.9.5: a) Measured TX output spectrum for the LTE Band2 (1.88GHz); b) Bandpass responses centered at different LOs. c) Power breakdown at different RF frequencies.

	This Work – TX-Mode	JSSC'14 [3]	ISSCC'15 [2]		
TX Techniques	SC Gain Loop + Gain-Boosted N-Path Filter + Wideband Push-Pull PAD	Current-Mode + Class-AB Power Mixer + Passive Baluns	Voltage-Mode Mixer + 33%-Duty-Cycle LO + Passive Baluns		
On-chip Balun/Inductor	Zero	Four	Two		
Multi-Band Flexibility	Defined by LO	Count on Baluns	Count on Baluns & Paths		
External Matching Parts	Zero (compatible w/ RX)	Zero (only TX)	Zero (only TX)		
Measured Performances at different LTE Bands (LTE10, 10MHz signal BW)					
	Band2 (1.88 GHz)	Band5 (0.836 GHz)	Band2 (1.88 GHz)	Band5 (0.836 GHz)	Band13 (0.782 GHz)
Output Power, P <sub>out</sub> (dBm)	-1	-1.2	3.1	2.8	2
Output Noise (dBc/Hz) @ freq. Offset (MHz)	-154.5 @ 80	-156 @ 45	-158 @ 80	-159 @ 45	-157.9 @ 31 (P <sub>out</sub> = -1dBm)
ACLR <sub>EUTRA1</sub> (dBc)	-40.3	-41.6	-43	-43.4	-54
ACLR <sub>EUTRA2</sub> (dBc)	-51.9	-50.3	-54.5	-54.9	N/A
EVM (%)	2.0	2.1	1.4	1.4	0.8
Power (mW)	38.4	31.3	69.6 <sup>b</sup>	73.6 <sup>b</sup>	216
TX Efficiency (%)	2.1	2.4	2.9	2.6	0.7
Active Area (mm <sup>2</sup> )	0.038		1.06 <sup>b</sup>		0.93
Supply Voltage (V)	1.1, 2.5		1.8		1.8
Technology (nm)	65		55 LP		40

<sup>a</sup> Measured with 50/20 Resource Block; <sup>b</sup> Without DAC, Biquad and 2 baluns given in [2] pp. 1636, Table 1

Figure 26.9.6: Measured TX-mode performance comparison.

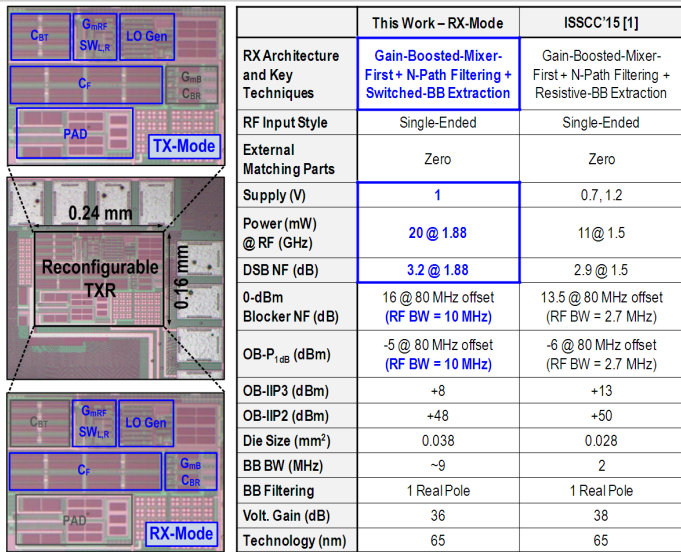


Figure 26.9.7: TXR die micrograph and its RX-mode performance comparison.